Available online at www.sciencedirect.com
ScienceDirect
Journal of Power Sources 168 (2007) 537–545
JOURNAL OF POWER SOURCES
www.elsevier.com/locate/jpowsour

Temperature effect on lifetimes of AMTEC electrodes

M.A.K. Lodhi [a,b,*], Justin B. Briggs [a]

[a] *Department of Physics, Texas Tech University, Lubbock, TX 79409, USA*
[b] *Department of Space Science, University of The Punjab, Lahore, Pakistan*

Received 30 November 2006; received in revised form 27 February 2007; accepted 28 February 2007
Available online 18 April 2007

Abstract

The alkali metal thermal to electric converter (AMTEC) is perhaps one of the most desirable devices for directly converting heat into electrical energy, particularly for deep space exploration, where time can be prolonged from a decade to a score of years. Its stability is expected to last for a long time, 15 years or more. The two major components responsible for power output of AMTEC are the electrolyte and the electrode. In this work, we describe research on the AMTEC electrodes, which might function without much power degradation as a function of time.

This study aims at performance of the electrodes by looking into the parametric changes of the material properties inherent to it with respect to time. These parameters refer to the grain growth involved in the grain mobility model for electrode materials. The grain size of some materials have been optimized for the least power degradation with respect to parameters characterizing the material properties. If the grain size of the electrode material reaches a certain dimension, about 500 nm, the power output starts degrading fast. The electrode materials studied in this work are molebdenum (Mo), titanium nitride (TiN), rhodium–tungsten alloys (RhW and Rh_2W). It was found that moybdenum electrodes have least power degradation for AMTEC designed for low temperature (<1100 K) operation. However, their grain growth is too rapid for operation above 1100 K. In that range of temperature for operating AMTEC rhodium–tungsten alloys are recommended.

Keywords: AMTEC electrode; Power degradation; Temperature-dependence

1. Introduction

Of the many new energy-converting devices the alkali metal thermal electric converter (AMTEC) is designed as a thermally regenerative, electrochemical device for the direct conversion of heat to electrical power. This machine requires a working liquid material to run through its interior. One of the main reasons for AMTEC being considered for space power is its high efficiency over other conventional thermal to electric converter. However, there is still some problem associated with its long and continuous use. Power output of the device is yet to perform consistently with time. During the testing of the PX-3A version of AMTEC in the laboratory, it was seen that power output decreased from 2.48 to 1.27 W after 18,000 h of operation with the hot side temperature of 1023 K and the condenser side temperature of 600 K [1]. There are several AMTEC cell models, the PX-type, tested at the U.S. Air Force Research Laboratory. Albuquerque, NM (AFRL). This study also focuses on the PX-3A cell. A description of the components of AMTEC is given in Tables 1 and 2 and their schematic arrangement in Fig. 1. The cell wall shields and contains the inner working components of the AMTEC system. Stainless steel is used as the wall material, which prevents heat loss through reflection. The hot plate is connected to the heat source to transfer heat to the cell. Additional conduction studs are added to increase heat transfer to the evaporator. The temperature at the hot side is maintained in the range of 1000–1300 K. The liquid sodium passes from the condenser through a wick to the evaporator, where it is converted to vapor, and enters beta" alumina solid electrolyte (BASE). The thermal rings, made of nickel are used to enhance the heat conduction between the support plate and the evaporator.

The BASE tubes are connected in an electrical series. Like the evaporator they are connected to a support plate. The cathode

* Corresponding author at: Department of Physics, Texas Tech University, Lubbock, TX 79409, USA. Tel.: +1 806 742 3778; fax: +1 806 742 1182.
E-mail address: a.lodhi@ttu.edu (M.A.K. Lodhi).

0378-7753/$ – see front matter © 2007 Elsevier B.V. All rights reserved.
doi:10.1016/j.jpowsour.2007.02.086

Table 1
Dimensions of the PX-3 A Cell

Mass	Length	Diameter	Volume	Heat sink/ heat source area	Length of base tube
0.147 kg	10.16 cm	3.175 cm	80 cm^3	7.9 cm^2	3.2 cm

Table 2
Design specifications of the PX-3A

Number of base tubes	Material of thermal rings	Condenser type	Evaporator type	Heat shield	Conduction stud
5	Nickel (0.11 cm thick)	CREARE	Conical	S.steel circumferential	Yes (0.38 cm^2)

electrode is applied on the BASE by chemical vapor deposition or sputtering techniques. The anode electrode is applied to the BASE by the Weber process and is covered with molybdenum mesh current collectors in order to prevent internal electric losses [2]. The thermal shield maintains prevention of parasitic heat loss as the hot end radiation eventually succumbs to the cold end [3]. The vapor eventually finds its way to the condenser, where it condenses to the liquid state and then flows down the wick [4].

The Tables 1 and 2 show dimensions and specifications for PX-3A AMTEC.

AMTEC does not have any moving parts [5–8] except for the sodium, which flows in a closed cycle as a working fluid. The BASE is the ionic conductor and divides the AMTEC into two regions; a hot region filled with sodium vapor at high-pressures (10–100 kPa) and high-temperatures (900–1300 K) and a cold region at low-pressures (<100 Pa) and low-temperatures (400–700 K) [9]. Fig. 2 shows the working principle of AMTEC. A porous metal electrode (cathode) covers the low-pressure (outer) side of the BASE. The anode surface covers the inner side of the BASE at the high pressure-temperature region of the cell (see Fig. 1). Both electrodes provide a conduction path for the electrons to and from the external load. Sodium enters the hot region of the cell. Due to the thermodynamic potential across the BASE, ionization of sodium metal occurs at the hot region of anode and BASE interface [10]. The sodium ions are diffused through the BASE to the cathode due to the pressure differential across the BASE. The electrons circulate through the external load producing electrical work and then reach the cathode surface, where they recombine with the sodium ions at the interface between the BASE and cathode. The neutralized sodium leaves the porous electrode, moves through the vapor space, and releases its heat of condensation on the condenser surface. Nearly the entire temperature drop occurs in this low-pressure vapor space. The condensed liquid sodium moves to the wick annulus to the inlet of a small dc electromagnetic pump or a porous capillary wick, which is used to return the sodium to the high-pressure evaporator region.

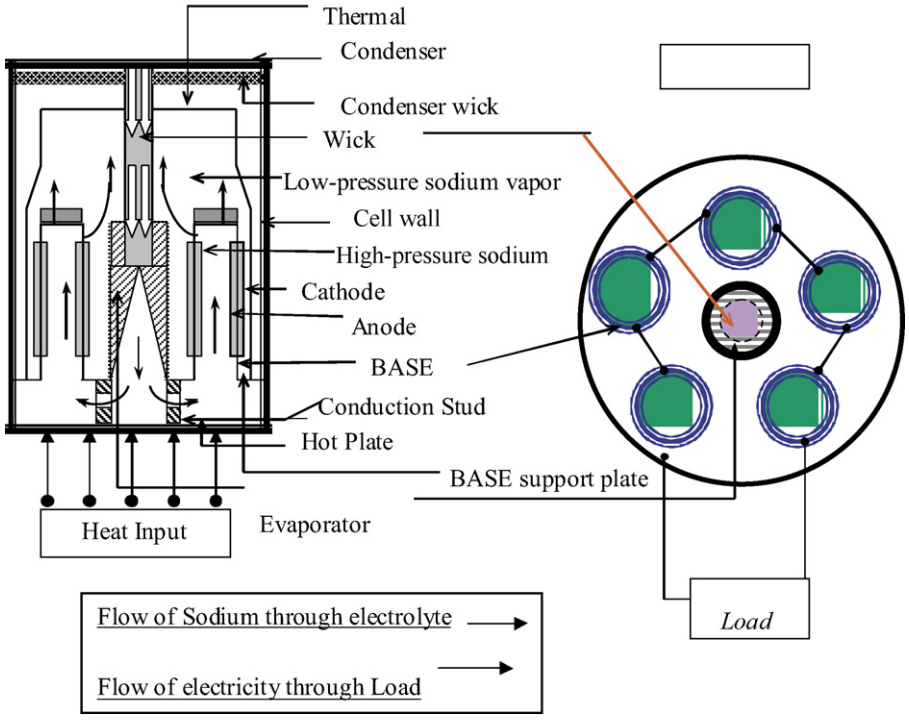

Fig. 1. Top and cross sectional views of the PX-3A cell.

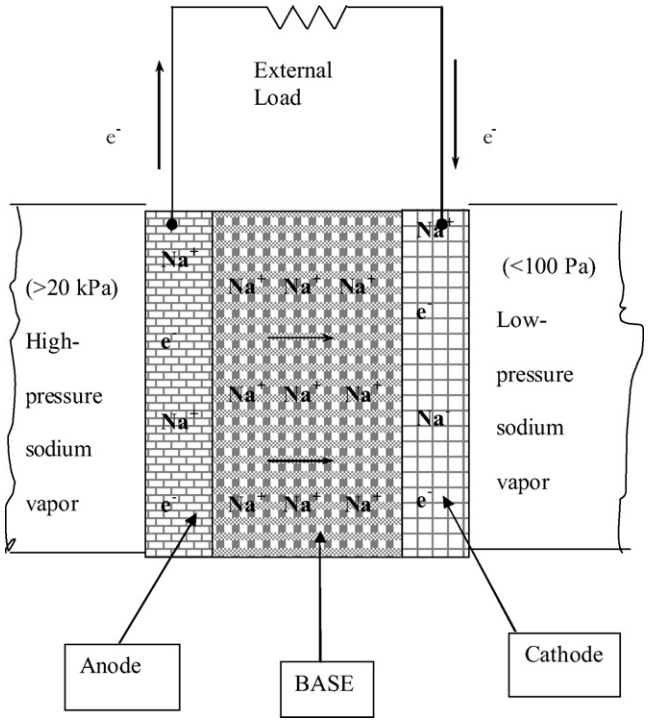

Fig. 2. Main parts and working principle of AMTEC cycle.

2. Electrode characteristics

The electrodes must have a suitable porosity and be stable under operating temperatures for certain desired period of time. It should be able to provide a site for the electrochemical reactions for sodium ionization and recombination of sodium ions and electrons. The electrode should be chemically and thermally compatible with the BASE and other components, to prevent corrosion. The sodium ions should be able to easily migrate from the high-pressure anode side to the low-pressure cathode side. The electrode should not be a barrier to the sodium ions. The electrons should be able to leave the anode site and travel to the load and recombine at the cathode to complete the circuit. The electrical conductivity of electrodes should be high enough to allow the electrons to move through the external circuit. The grain of the electrode should coalesce very slowly in order to prevent voids from appearing. The electrical conductivity decreases as the voids open up. Electrode materials, used should have high melting point in order to have a lower surface diffusion coefficient. This corresponds to low sintering of the electrode grains. It is important that the electrode does not alter its physical morphology during the long hours of operation [11]. The electrode material in contact with the BASE material should have a high tolerance to thermal expansion. Ceramic electrodes have a lower tolerance compared to the metal electrodes. The negative Gibbs free energy should be large enough to prevent material loss due to dissociation.

The electrode performance greatly depends on its material [12]. The electrical resistance, thermal expansion coefficient, vapor pressure, and surface self-diffusion coefficients are the most desired parameters in selection for the material for electrode construction. The electrical resistance and the surface self-diffusion should be low for an ideal electrode. Also the thermal expansion coefficient of the electrode should be very similar to the BASE material.

The triple phase boundary involves the electrode, BASE, and sodium interaction where a longer triple phase boundary is the result of a finer grain size [13]. Also the charge transfer process occurs at the triple phase boundary. If the length of the triple phase boundary increases, the over-voltage decreases. Then the electrode with a finer grain size will obtain higher current densities.

3. Effect of grain growth of electrode materials on power output

Recent study shows that BASE and electrodes are two of the most power degrading components in the AMTEC [14,15]. The lifetime of AMTEC electrodes is dependent on the sintering rate of the material, which, in turn depends on the operating temperature of the cell and inherent properties of the material. The time for which the performance of the electrode is satisfactory to produce adequate power output for the AMTEC system is defined as the electrode lifetime. If the electrode grains grow to a diameter of 1000 nm (some limit to 500 nm) then they cease to function properly [16]. The sintering rate of the electrode material is a function of the operating temperature of the cell thus the operable lifetime of an AMTEC electrode is temperature-dependent [16]. As grains sinter, they coalesce, resulting in an increase in the grain volume. The grains coalescing process increases the porosity of the electrode material and causes the contact surface area of the electrodes with BASE to decrease. The performance of the electrode is related to the contact between electrode and electrolyte, which is measured by temperature independent exchange current or just exchange current. The exchange current depends on the operating fluid pressure at the interface of electrolyte and electrode. The pressure at the interface is the sum of the pressure caused by the condensation of metal vapor from the condenser, the pressure due to the metal vapor leaving the exterior surface of the electrode, and the pressure drop from the electrode–electrolyte interface to the electrode surface. Therefore, temperature independent exchange current is a sensitive measure of the nature of contact between electrode and electrolyte interface. It can also be related with the operable lifetime of the electrode through grain size.

With an increase in sintering, grain size increases, which eventually leads to a decrease in the number of grains. Therefore, contact between electrolyte and electrode also decreases. As the total number of grain decreases, the exchange current also decreases, because the exchange current is proportional to the number of grains in the electrode. With the increase of grain size, voids within the electrode become larger which causes the electrode conductivity to decrease. Eventually, these voids will grow to a huge size that there will be no apparent grain-to-grain conduction and the effective lifetime of electrode will reach its end eventually.

In brief when the electrodes are exposed to sodium under high pressure and temperature they tend to sinter, thus affecting the

porosity, resistance, the nature of grains and the contact of electrodes with the BASE. Voids or porous holes in the electrodes are formed, which allows the sodium to flow through them easily. The voids will increase after an extended period of time. This reduces the grain-to-grain contact, dropping the electrical conductivity, and ultimately disables the electrodes to function any further.

4. Grain boundary mobility model

The grain growth of the electrode is due mainly to material diffusing between adjacent grains. The surface contact among the electrode grains is reduced as the grains grow and thus degrade the performance of the electrode. The neighboring grains continue to merge into each other until the surface energies related to the tension between the grains becomes balanced. This condition arises when the grains cannot grow any further because the other grains confine them and they rid their strained energy state by coalescing with other grains.

The grain growth takes place with kinetics where the adjacent grain boundaries have a net motion with respect to each other. The pressure difference or driving force at the grain boundary with a constant called the mobility factor is related to the velocity of the grains given by [17]:

$$V = M\Delta P \tag{1}$$

where M is mobility factor and ΔP is pressure difference. The pressure difference can be approximated with the average grain radius, R assuming it to be a spherical drop and the average grain boundary energy γ_b (surface tension) from the well known relation:

$$2\pi R\gamma_b = \pi R^2 \Delta P \quad \text{or} \quad 1/2\Delta P = \gamma_b/R \tag{2}$$

The boundary velocity is as follows:

$$V = \frac{dR}{dt} = M\Delta P = \frac{2M\gamma_b}{R} \tag{3}$$

Rearranging and solving in terms of R the equation becomes

$$R^2 - R_o^2 = 4M\gamma_b t, \tag{4}$$

where R_o is the initial grain radius.

The quadratic grain growth variation of the radius given by Eq. (4) has been derived under ideal conditions. However, the actual pressure difference at the grain boundary has a more complex dependence upon the surface and volume energies at the grain boundary resulting in a higher order of dependence on R in practice and thus may vary from material to material. For a more practical aspect the Eq. (4) may be replaced by a more general equation [17]:

$$R^n - R_o^n = cM\gamma_b t \tag{5}$$

where n is the grain growth exponent to be evaluated and c the proportionality constant to give correct dimensions. Since there is no hard and fast rule for the number n, it is used as an experimentally determined parameter for different materials and possibly different physical conditions for the electrode to operate. Accordingly, this parameter will be considered as a free parameter to obtain the optimal results for different materials.

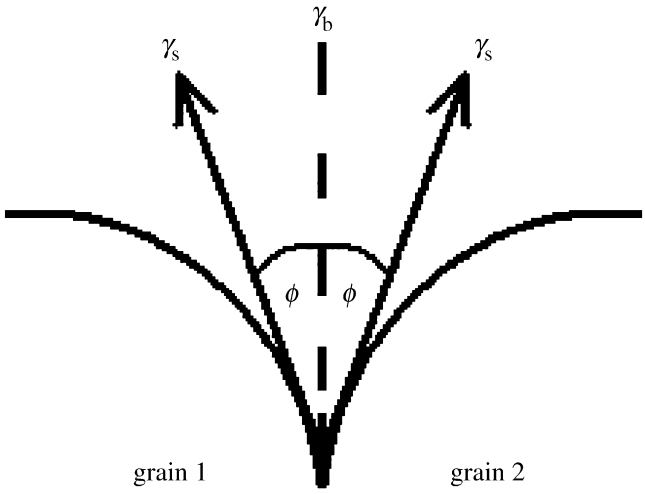

Fig. 3. Diagram of the boundary energy arising from the contact of two grains.

The mobility factor, M obeys Arrhenius relation because the mobility of grain boundaries increases as temperature increases, with specified activation energy E_A. The relationship between the rate a reaction proceeds and its temperature is determined by the Arrhenius relation. At higher temperatures, the probability of the neighboring grains will merge together is higher. The activation energy is the amount of energy required to ensure that this reaction happens. The mobility factor is defined as [17]:

$$M = M_o \exp\left(-\frac{E_A}{R_g T}\right) \tag{6}$$

where M_o is the mobility constant, T the temperature on the hot side, and R_g here is used for gas constant. After the substitution for M from (6) into Eq. (5) the following equation,

$$R^n - R_o^n = tcM_o \exp\left(-\frac{E_A}{R_g T}\right)\gamma_b, \tag{7}$$

represents the grain growth as a function of activation energy, time and temperature.

The boundary energy, γ_b, defined as the minimum amount of energy needed to bond two-grain boundaries or break them apart, and can be ascertained by adding the components of the surface energy of the grains at the interface. The surface tension and pressure forces at the grain boundary produce an angle ϕ, see Fig. 3, between the individual grain boundaries, so that

$$\gamma_b = 2\gamma_s \cos\phi \tag{8}$$

By substituting Eqs. (8) into (7) gives the equation that describes grain size dependent upon time and temperature as [18]:

$$R_f = R_o\left[1 + \frac{(2cM_o\gamma_s \cos\phi)t \exp(-E_A/R_g T)}{R_o^n}\right]^{1/n} \tag{9}$$

Here a new parameter "a" called the mobility parameter, to be determined, is introduced defined by:

$$a = 2cM_o\gamma_s \cos\phi \tag{10}$$

The Eq. (9) with (10) thus becomes

$$R_f = R_o\left[\frac{1 + at\ \exp(-E_A/R_gT)}{R_o^n}\right]^{1/n} \tag{11}$$

The effect of altering parameter "a" ($2cM_o\gamma_s \cos\phi$), in the grain growth equation alters the behavior of the grain size for different materials. This expression demonstrates that as "a", increases, R increases also. The parameters $2c$, M_o, γ_s, and $\cos\phi$ on which parameter "a" depends cannot be easily measured in a laboratory setting [16]. It is, however, assumed that M_o and γ_s are temperature dependent but only weakly compared with E_A, thus these parameters are assumed to be constant. The angle ϕ, between grains, is weakly dependent upon time and will also be assumed constant [16].

The effect of altering n, the growth exponent, in the grain growth equation alters the behavior of the grain size for various materials. The experimental value for n has been determined between 3 and 6.5 depending upon the material. If the grain growth of the material is regulated more by volume diffusion than surface diffusion at the grain boundary then it will be closer to 3. If the grain growth of the material is regulated more by surface diffusion than volume diffusion at the grain boundary then it will be closer to 4. This demonstrates that as n increases, R decreases. Since power degradation is dependent upon increasing of the grain size, the choice of material with higher n should lessen the grain growth over time and keeps the power degradation low.

The effect of altering the temperature T, of the electrode on the hot side, in the grain growth equation alters the behavior of the grain size for different materials. This specific T corresponds to the hot side of the AMTEC device where the electrode is exposed to high temperature and pressure. This demonstrates that as T increases, R increases.

The effect of varying activation energy in the grain growth equation alters the behavior of the grain size for different materials. The activation energy is the amount of energy that is needed to allow the grain boundaries to begin expanding within the material. Conceptually, this tells us that the higher the activation energy a material has, the slower the grain will grow over time due to a larger energy barrier to grain boundary expansion.

The function of the electrodes and the role played by their various components is to be determined in order to understand the time-dependent behavior of AMTEC electrodes. One can calculate the grain size dependence upon time, temperature independent exchange current and power output for the electrode. By:

1. Applying the grain boundary mobility growth model to various materials, like; molybdenum (Mo), titanium nitride (TiN), and rubidium tungsten alloys (RhW) and (Rh_2W).
2. Studying the effect of changing the parameter "a" in the grain growth model to observe the behavior of the grain size for aforementioned materials.
3. The effect of altering activation energy (E_A) in the grain growth model to observe the behavior of the grain size for materials chosen.
4. Varying the growth exponent (n) in the grain growth model to observe the behavior of the grain size for those materials.
5. Changing the temperature (T) of the electrode on the hot side, in the grain growth mode to observe the behavior of the grain size for subject materials.

5. Relation between grain size, exchange current and power output

The temperature independent exchange current is a measure of the efficiency of the ionization of the sodium vapor carried out at the anode/electrolyte interface. The electrons are transferred to the electric lead to supply power from the AMTEC system to the load while the sodium ions traverse through the BASE to recombine with the electrons at the interface of electrolyte/cathode to travel to the condenser and repeat the process.

The Jet propulsion Laboratory, Pasadena, CA (JPL) has done experimental studies of grain growth rates for various materials and has created an empirical relation between grain size of electrode materials and temperature independent exchange current given by [13]:

$$B = B_o - bR_f^{1/2}, \tag{12}$$

where B is the temperature independent exchange current (or exchange current) and B_o is initial temperature independent exchange current, assumed to be ($270\,AK^{1/2}\,m^{-2}\,Pa^{-1}$) and b is the coefficient of electrode exchange current pertaining to the material used and is determined experimentally as 6.218.

It is important to realize that this empirical relation is based on the measured behavior of Mo, platinum-tungsten (PtW), and RhW electrodes. JPL has reported that they do not know if Eq. (12) would be applicable to TiN electrodes [16]. Although one thing is for sure that the grain size of the electrode will increase as the reaction zone decreases between the electrode and electrolyte, thus the temperature independent exchange current will decrease [16].

If the temperature independent exchange current is known, the power output of AMTEC can be calculated. JPL has developed a semi-empirical plot of power output with respect to temperature independent exchange current [18]. It can be seen in Fig. 4 from the JPL model that AMTEC electrode power falls off slowly with temperature independent exchange current until it reaches far below its original value. When it falls far below its initial value, it is likely that voids have opened wide in the electrodes, the grains cannot have contact with each other, and hence the power output drops significantly.

It may be noticed that a decrease to 25% of the initial value of B corresponds to 70% of the initial value of power output the power output falls sharply when B goes down to 20% of its initial value. From the APEAM code the power output of the AMTEC cell is maximum when the value of B is 270, we use this initial value for the JPL model as well to compare the behavior of these two models, shown in Fig. 4. From the JPL

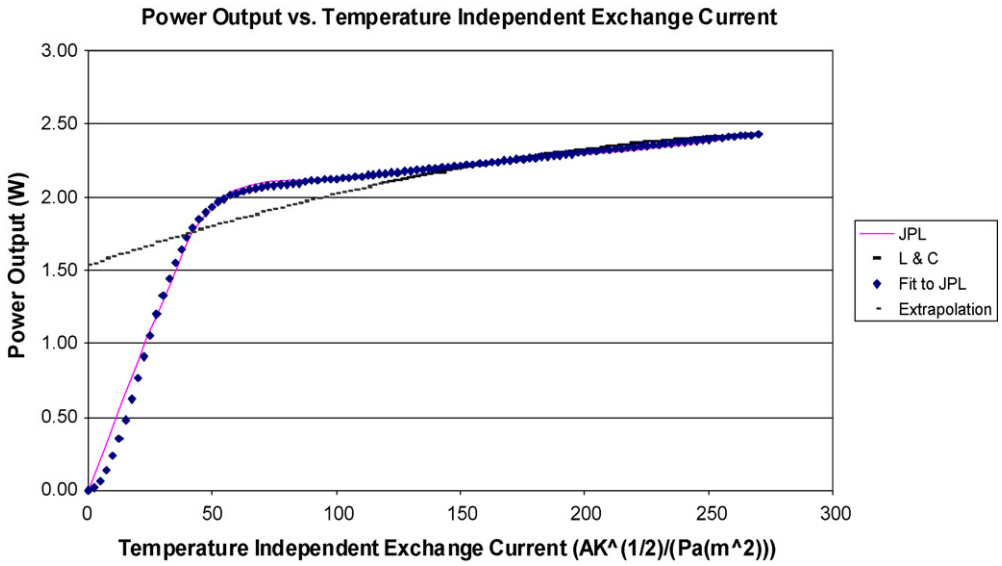

Fig. 4. Power Output vs. temperature independent exchange current for the JPL empirical model, fit to JPL and the Lodhi–Chowdhury model.

empirical plot [18] we have generated a mathematical relation between power output P_e and B given by:

$$P_e = 1.95(1 - e^{-B^2/850}) + 0.00178B \quad (13)$$

which is also plotted in Fig. 4 as a fit to JPL extrapolation in excellent agreement with the JPL original plot. When B goes down far below where power output P_e reaches its maximum value the P_e–B relation becomes unrealistic [19].

A simulation study by Lodhi and Chowdhury was performed to investigate the effect on the power output by varying the temperature independent exchange current within the realistic range of practical use [19] given by:

$$P_e = 1.5135 + 0.006 \times B - B^2 \times 10^{-5}. \quad (14)$$

For comparison this relation has also been plotted in Fig. 4 labelled as L&C curve and extrapolated to reach the zero value of B. This is in good agreement with the JPL and fit to JPL within the realistic range but has no correspondence with them below the lower range, 120 of B, The Lodhi–Chowdhury curve does not have the power truncation for lowers values of B in the unrealistic range of 120–0. The only difference between the two models, the JPL and Lodhi–Chowdhury models, is the behavior of the curves at lower values of B, between 0 and 120. The reason for this is that, unlike the JPL model, there is no truncation in the power output in the Lodhi–Chowdhury model as B approaches 0 from a value of 120. Since the Lodhi–Chowdhury formula is fitted for the relevant range of B, it should therefore not be extrapolated beyond the range of B they used in their algorithm.

Fig. 5, obtained from Eq. (14) relates the power output of AMTEC to the temperature independent exchange current within the range of 120–280. This is the range of practical use and should not be extrapolated beyond [19].

6. Optimization of the power output

By substituting for B from Eq. (12) into equation (14) gives:

$$P_e = 1.5135 + 0.006\,(B_o - bR_f^{1/2}) - (B_o - bR_f^{1/2})^2 \times 10^{-5}. \quad (15)$$

The Eq. (15) gives a direct relationship of the power output of AMTEC and the grain size of electrode material, characterized by parameters a, E_A and n, depending on time and temperature.

The optimal value of the grain size in term of the temperature independent exchange current for an electrode material can be found by differentiating power in Eq. (15) with respect to grain size.

$$\frac{\partial P_e}{\partial R_f} = R_f^{-1/2}(-0.003b + 1 \times 10^{-5} b B_o) - 1 \times 10^{-5} b^2 = 0 \quad (16)$$

Simplifying and solving for R_f yields the following result:

$$R_f = \left(\frac{0.003 \times 10^5 - B_o}{-b}\right)^2 = \left(\frac{B_o - 300}{b}\right)^2 \quad (17)$$

This equation calculates a value for R_f for a given B_o. The initial grain radius R_o corresponds to a specific value of B_o where the AMTEC performance for the power output is ideally maximized.

7. Result

The calculated values of R_f for various values of B_o are given in Table 3. The power output of the AMTEC cell is maximum when B_o is 270 $AK^{1/2}\,m^{-2}\,Pa^{-1}$ according to the APEAM code

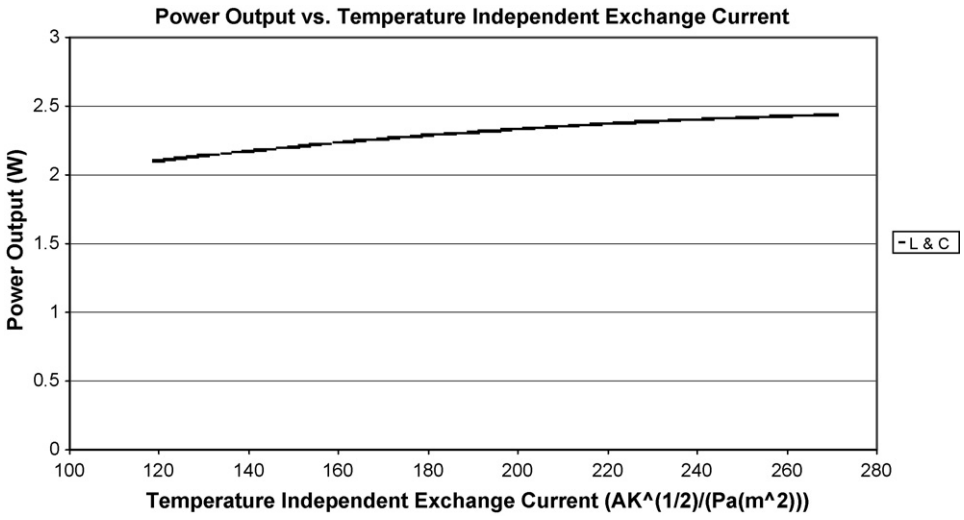

Fig. 5. A simulated plot of the power output with respect to B from Eq. (13).

[20]. This value of B_o ($270\,AK^{1/2}\,m^{-2}\,pa^{-1}$) corresponds to a value of 23 nm for R_f in Table 3. Value of B, higher than $270\,AK^{1/2}\,m^{-2}\,pa^{-1}$, are also used to calculate the corresponding values of R_f. For example, B_o equal to $290\,AK^{1/2}\,m^{-2}pa^{-1}$ corresponds to a value of R_f equal to 3 nm (see Table 3.) This value however, is less than the value of R_o for any material considered in this study, we therefore regard such values unphysical. However, it is desirable to look for a grain size of the electrode as small as possible to increase B and thus the power output. The grain sizes of different electrode materials have been measured by JPL to give an initial idea of what the temperature independent exchange current should be [16]. The grain size of materials R_f of TiN, RhW, Rh_2W, and Mo are given 30, 5, 5, and 10 nm, respectively [13]. These sizes correspond to atemperature independent exchange current, for those materials as $266\,AK^{1/2}m^{-2}\,Pa^{-1}$ $286\,AK^{1/2}m^{-2}\,Pa^{-1}$, $286\,AK^{1/2}m^{-2}\,pa^{-1}$, and $280\,AK^{1/2}m^{-2}\,Pa^{-1}$ (see Table 3). Using the APEAM code,

Table 3
The optimized grain size for corresponding values of temperature independent exchange current

Initial temperature independent exchange current ($AK^{0.5}\,Pa^{-1}\,m^{-0.5}$)	Grain size (nm)
50	1617
70	1368
90	1141
80	1252
110	934
130	747
150	582
170	437
190	313
210	209
230	127
250	65
266	30
270	23
280	10
286	5
290	3

Table 4
The temperature independent exchange current, percentage deviation, and power output for different materials

	Mo	RhW	Rh_2W	TiN
Grain size meas [16] (nm)	10	5	5	30
Grain size calc (nm)	23	23	23	23
Temp. ind. exchange current (APEAM)	270	270	270	270
Temp. ind. exchange current (this work)	280	286	286	266
% Deviation in B	3.70	5.90	5.90	1.48
Power output (W)	2.19	2.23	2.23	2.11

Table 5
Least power degradation % for materials by varying single parameter

	n	a	E_A	T
Overall	3–11	3–12	1–7	11–22
Mo	3 (6.5)	12 (9.57E38)	7 (950)	15 (1050 K)
TiN RhW	11 (4.0)	3 (2.26E08)	2 (275)	22 (1050 K)
	8 (4.0)	3 (4.60E10)	1 (325)	11 (1050 K)
Rh_2W	8 (4.0)	3 (1.82E08)	1 (275)	12 (1050 K)

which corresponds to the grain size of 23 nm, the power is maximized with a value of B_o equal to $270\,AK^{1/2}m^{-2}\,Pa^{-1}$. It is interesting to compare this value with the calculated R_f values given in Table 3. This comparison is given in Table 4. As R_f increases with time, the temperature independent exchange current B decreases.

The power degradation by varying individual parameters and keeping others constant at an optimum level has been studied.

Table 6
Worst power degradation % for materials by varying single parameter

	n	a	E_A	T
Overall	19–37	24–67	19–59	25–100
Mo	20 (4.0)	67 (9.57E42)	59 (700)	100 (1250 K)
TIN	37 (3.0)	46 (2.26E12)	50 (150)	43 (1250 K)
RhW	19 (3.0)	24 (4.60E14)	19 (200)	27 (1250 K)
Rh_2W	20 (3.0)	25 (1.82E12)	19 (150)	25 (1250 K)

Table 7
Optimal values of ideal electrode parameters that minimize power degradation operating at 1050 K for 15 years

Electrode material #	Initial grain radius R_o (nm)	Parameter "a"	Activation energy E_A (kJ/mole)	Grain exponent n
1	5	1.82E + 08	275	4.0
2	5	4.60E + 10	325	4.0
3	10	9.57E + 38	950	6.5
4	30	2.26E + 08	275	4.0

Table 8
Power degradation and efficiency of real materials

Electrode material	Power degradation 1050 K (%)	Power degradation 1150 K (%)	Efficiency initial/final 1050 K (%)	Efficiency initial/final 1150 K (%)
Mo	6.5	28.7	12.2/11.4	12.2/8.7
RhW	10.3	18.3	12.6/11.3	12.6/10.3
Rh_2W	11.9	18.3	12.6/11.1	12.6/10.3
TiN	22.3	32.1	11.2/8.7	11.2/7.6

They are summarized in Tables 5 and 6 for the best and worst scenarios. The quantities within the parentheses in Tables 5 and 6 are for the values of the respective parameters which give the power degradation percentage in that particular box.

Table 7 show the optimal values of grain growth parameters which yield the ideal power output with zero power degradation over a period of 15 years of operation at temperature 1050 K. We also calculated the efficiency of the AMTEC cell for those ideal parameters. Also, the respective power output and efficiency are calculated for real materials whose grain growth parameters are close to the ideal ones for the same period. This comparison of power outputs and efficiencies of an ideal case and real materials are given in Tables 7 and 8, respectively.

8. Concluding remarks

The optimum performance of AMTEC has been accomplished by investigating into the behavior of the grain size of electrode materials by optimizing the performance of the electrodes. The power output of AMTEC cell is greatly affected by the choice of electrode materials. Since our objective is to use AMTEC for a long period of time, we have therefore investigated for conditions that least affect the degradation of power output, when used for a long time. The power degradation is strongly coupled with the growth of the grain size of the electrode materials. We found that grain growth is sensitive to the parameters, like initial grain size, mobility parameter "a", exponent growth parameter n, activation energy E_A, temperature of the hot side of the AMTEC cell, T and the time of operation, t.

This study focused on the performance of the electrode by adjusting certain conditions that are inherent to the electrode materials with respect to time. These conditions are grain growth parameters involved in the grain mobility model for electrode material. If the grain size of the electrode material reaches a certain dimension, about 500 nm, it no longer functions properly. This is very important because this condition should not occur until after the time desired for operation. For a period of 15 years it corresponds to a power degradation percentage of 25 to 30% overall for different electrode materials.

The power degradation has been minimized with respect to parameters for an ideal case is minimum for ideal parameters and also for real materials, which is found to be rather small, varying of course from material to material. This work establishes the electrode materials performance for power output and efficiency in the descending order, of Mo, RhW, Rh_2W, and TiN when operated at a temperature of 1050 K. However, if the tempertatue is raised to 1150 K the order is changed to RhW, Rh_2W, Mo and TiN, for both power output and efficiency. This leads to the conclusion that the power degradation of Mo is highly sensitive to the temperature of operation of the hot side of the AMTEC cell compared to the other three materials investigated in this work. This is evident from Table 8, which shows the power degradation and efficiencies at temperatures 1050 and 1150 K. Moybdenum electrodes have least power degradation for AMTEC designed for low temperature (less than 1100 K) operation. However, their grain growth is too rapid for operation above 1100 K. In that range of temperature for operating AMTEC rhubidium-tungsten alloys are recommended, see Table 8.

A formula, given by Eq. (13) has been generated for the JPL model curve which demonstrates the relationship between power output and the temperature independent exchange current. It is seen that the power output falls very slowly until reaching a certain percentage of the initial value of B, about 20%, then begins to decrease quickly until it reaches zero. The JPL model curve, the curve obtained from Eq. (13), and that of the Lodhi–Chowdhury algorithm for power output as the function of the temperature independent exchange current B, in Fig. 4, agree very well except for the low values of B.

It is because the Lodhi–Chowdhury model is fitted for a certain range of B which is of practical use for power output in the AMTEC cell. To extrapolate this model beyond the chosen range would be erroneous.

References

[1] Merrill, John, AFRL, private communication.
[2] M.A. Ryan, et al., in: M.S. El-Genk (Ed.), Space Technology and Applications International Forum, AIP Conf. Proc 458, American Institute of Physics, NY, 1999, pp. 1301–1305.

[3] C.A. Borkowski, R.C. Svedberg, T.J. Hendricks, Intersociety Energy Conversion Engineering Conference, vol. 2, 1997.
[4] M.S. El-Genk, J.M. Tournier, in: M.S. El-Genk (Ed.), Space Technology and Applications International Forum. AIP Conf. Proc 420, American Institute of Physics, NY, 1998, pp. 1586–1594.
[5] T.K. Hunt, N. Weber, T. Cole, Proceedings of the 13th Intersociety Energy Conversion Engineering Conference, SAE, Warrendale, PA, 1978, p. 2011.
[6] R. Mital et al. Performance Evaluation of Gas Fired AMTEC Power Systems, Advance Modular Power Systems, Inc., USA, reports 1–2, 1998.
[7] M.A. Ryan, et al., J. Electrochem. Soc. 142 (1995) 4252–4256.
[8] R.K. Sievers, C.P. Bankston, 23rd Intersociety Energy Conversion Engineering Conference, IECECT, 1988, p. 3.
[9] R.M. Williams, et al., J. Electrochem. Soc 137 (1990) 1709–1715, Honolulu, HI.
[10] T. Cole, Science 221 (1983) 915–920.
[11] M.A. Ryan, R.M. Williams, M.L. Underwood, J.-N. Barbara, D. O'Conner, in: M.S. El-Genk (Ed.), Space Technology and Applications International Forum, AIP Conf. Proc 271, American Institute of Physics, NY, 1993, pp. 905–912.
[12] B. Fiebig, M. Schuller, M. Amy Ryan, R. Williams, P. Hudsov, in: M.S. El-Genk (Ed.), Space Technology and Applications International Forum, AIP Conf. Proc 458, American Institute of Physics, NY, 1999, pp. 1312–1318.
[13] T.K. Hunt, et al., in: Proc. Second Symp. on Electrode Mat. And Processes for Energy Conversion and Storage, vol. 87–112, J. Electrochem. Soc. (1987) 608.
[14] M.A.K. Lodhi, P. Vijayaraghavan, A. Daloglu, J. Power Sources 93 (2001) 41.
[15] M.A.K. Lodhi, M.S. Chowdhury, J. Power Sources 96 (2001) 369.
[16] M.A. Ryan, et al., in: M.S. El-Genk (Ed.), Space Technology and Applications International Forum, AIP Conf. Proc 504, NY, American Institute of Physics, 2000, pp. 1377–1382.
[17] V.B. Shields, et al., Intersociety Energy Conversion Engineering Conference, NY, 1999, pp. 1–3.
[18] M.A. Ryan, A. Kisor, R.M. Williams, B. Jeffries-Nakamura, D. O'Connor, 29th Intersociety Energy Conversion Engineering Conference, IECECT, 1994, pp. 877–881.
[19] M.A.K. Lodhi, M.S. Chowdhury, J. Power Sources 103 (2001) 18–24, Elsevier.
[20] J.-M.P. Tournier, M.S. El-Genk, in: M.S. El-Genk (Ed.), Space Technology and Applications International Forum, AIP Conf. Proc 420, American Institute of Physics, NY, 1998, pp. 1576–1585.